Molecular Cloning and Developmental Expression of the Caveolin Gene Family in the Amphibian *Xenopus laevis*[†,‡]

Babak Razani,[§,||] David S. Park,[§,||] Yuko Miyanaga,[⊥] Ashwini Ghatpande,[⊥] Justin Cohen,[⊥] Xiao Bo Wang,[§,||] Philipp E. Scherer,[@] Todd Evans,[⊥] and Michael P. Lisanti*[,§,||]

Department of Molecular Pharmacology, Albert Einstein College of Medicine, 1300 Morris Park Avenue, Bronx, New York 10461, The Division of Hormone-Dependent Tumor Biology, The Albert Einstein Cancer Center, 1300 Morris Park Avenue, Bronx, New York 10461, Department of Developmental and Molecular Biology, Albert Einstein College of Medicine, 1300 Morris Park Avenue, Bronx, New York 10461, and Department of Cell Biology, Albert Einstein College of Medicine, 1300 Morris Park Avenue, Bronx, New York 10461

Received January 16, 2002; Revised Manuscript Received April 26, 2002

ABSTRACT: Caveolae are ∼50−100 nm invaginations of the plasma membrane thought to form as a result of a local accumulation of cholesterol, sphingolipids, and a unique family of three proteins known as the caveolins: Cav-1, -2, and -3. Here, we report the identification, sequence, and developmental expression of the three caveolin genes in the amphibian *Xenopus laevis*. Sequence comparisons show that *Xenopus* Cav-1, -2, and -3 are ∼80, 64, and 45% identical, respectively, to their counterparts in humans. Furthermore, Northern blotting experiments demonstrate that the *Xenopus* caveolins have tissue-specific expression profiles consistent with those previously reported in adult mammals. In the adult frog, *Xenopus* Cav-1 and Cav-2 are most abundantly expressed in the fat body and the lungs, while *Xenopus* Cav-3 is primarily expressed in muscle tissue types (heart and skeletal muscle). However, our temporal and spatial analyses of these expression patterns during embryogenesis reveal several novel features, with possible relevance to developmental signaling. Transcripts encoding *Xenopus* Cav-1 and -2 first appear in the notochord of neurula stage embryos, which represents a key signaling tissue. In contrast, *Xenopus* Cav-3 shows a highly specific punctate expression pattern in the embryonic epidermis, similar to previous patterns implicated in Notch signaling. These findings are in striking contrast to their steady-state expression patterns in the adult frog. Taken together, our results show that the *Xenopus* caveolin gene family is present and differentially expressed in both embryonic and adult tissues. This report is the first detailed study of caveolin gene expression in a developing embryo.

Palade and Yamada first coined the terms *plasmalemmal vesicles* and *caveolae* to describe conspicuous 50−100 nm invaginations of the plasma membrane which resemble "little caves" on transmission electron microscopy (TEM). Indeed, caveolae are clearly distinct in morphology from the more electron-dense and much larger (∼250−300 nm) clathrin-coated pits (*1*, *2*). The definition of caveolae has since broadened to also include individual or grapelike clusters of 50−100 nm vesicles detached from the plasma membrane proper. Regardless of the form in which they are found, caveolae have several important characteristics. In general, caveolae are considered a subset of membrane entities known as lipid rafts (*3*, *4*). Whereas the plasma membrane is mostly composed of phospholipids that exist in a fluid "liquid-disordered" state, lipid rafts form via a coalescence of cholesterol and sphingolipids which imparts a more rigid "liquid-ordered" assembly. As a result, lipid rafts and caveolae are less dense than their phospholipid counterparts and have the unusual distinction of being resistant to solubilization by mild nonionic detergents, such as Triton X-100 at 4 °C. What distinguishes caveolae as a specialized form of lipid raft is their selective association with a specific family of membrane proteins, the caveolins (*4*).

Caveolin, the original member of a three-protein caveolin family, was first identified as a major phosphorylated protein in v-Src transformed cells (*5*). Antibodies raised against this 22 kDa protein were subsequently found to decorate exclusively the cytoplasmic face of caveolae membranes, thereby identifying caveolin (now called caveolin-1) as the first bona fide protein marker of caveolae (*6*). Since then, two other members of the caveolin family have been discovered (caveolin-2 and -3) and shown also to target exclusively caveolae microdomains (*7*, *8*). In this respect, the expression patterns of caveolins-1, -2, and -3 fully correlate with the presence of caveolae in those tissues. Interestingly, the

[†] This work was supported by grants from the National Institutes of Health (NIH), the Muscular Dystrophy Association (MDA), and the American Heart Association (AHA) (to M.P.L.) and the National Institutes of Health (to T.E.). B.R. was supported by a NIH Medical Scientist Training Grant (T32-GM07288) and D.S.P. by a NIH Graduate Training Program Grant (TG-CA09475).

[‡] The three cDNA sequences reported in this paper have been deposited in GenBank with accession numbers AF455042, AF455043, and AF455044.

* To whom correspondence should be addressed. Telephone: (718) 430-8828. Fax: (718) 430-8830. E-mail: lisanti@aecom.yu.edu.

[§] Department of Molecular Pharmacology, Albert Einstein College of Medicine.

[||] The Division of Hormone-Dependent Tumor Biology, The Albert Einstein Cancer Center.

[⊥] Department of Developmental and Molecular Biology, Albert Einstein College of Medicine.

[@] Department of Cell Biology, Albert Einstein College of Medicine.

10.1021/bi020043n CCC: $22.00
Published on Web 06/01/2002

expression patterns of caveolin-1 and -2 are in large part distinct from that of caveolin-3. Whereas adipocytes, endothelial cells, pneumocytes, and fibroblasts have the highest levels of caveolin-1 and -2, caveolin-3 expression is limited mainly to muscle cell types (i.e., cardiac, skeletal, and smooth muscle cells) (*7*−*10*).

Over the past few years, it has become increasingly apparent that caveolar function is in large part dependent on the presence of the caveolins. The caveolins mediate the formation of caveolae in vivo (*11*, *12*). Furthermore, caveolae and the caveolins have been implicated in various endocytic processes, cholesterol trafficking and homeostasis, signal transduction, oncogenesis, and muscular dystrophy (reviewed in ref *13*). Thus far, the prime focus of caveolae/caveolin research has been in mammalian systems; this has led to the molecular cloning and detailed characterization of several mammalian caveolins (*7*, *8*, *14*). To exploit experimental advantages in other model organisms, the discovery of homologous nonmammalian caveolins and their characterization will be extremely valuable. For example, expressed sequence tag (EST) searches of *Caenorhabditis elegans* databases led to the molecular cloning of the caveolin homologues in this widely studied genetic organism (*15*). In turn, Kurzchalia and colleagues used this information to ablate the expression of *C. elegans* caveolin-1 via an RNAi antisense strategy and found very intriguing abnormalities in the meiotic cell cycle (*16*).

Stemming from the extreme utility of electron microscopy in the understanding of cellular architecture, the literature is replete with reports of tissues containing various levels of caveolae. Interestingly, several of these early studies were conducted on frog organ systems, including the intestinal tracts, skeletal and cardiac muscles, and the vasculature (*17*−*22*), indicating that caveolar microdomains are abundant in adult frog tissue and show a pattern of expression similar to that seen in mammals.

Given that the frog has served as a valuable model experimental organism for both biochemical and developmental studies, we set out to identify the caveolar marker proteins for these microdomains, the caveolins, in *Xenopus*. Here, we report the molecular cloning of the three members of the caveolin gene family in *Xenopus laevis*. In addition, we present a detailed analysis of their expression patterns in the developing and adult frog using Northern blot analysis and *in situ* hybridization techniques. This report is the first detailed analysis of the spatial and temporal expression patterns of the caveolin genes in a developing embryo.

EXPERIMENTAL PROCEDURES

Xenopus Embryos. Xenopus female frogs were induced to lay eggs by injection with 800 units of human chorionic gonadotropin. Eggs were fertilized in vitro using a sperm suspension, de-jellied in 2% cysteine hydrochloride (pH 7.8), and rinsed in 0.1× Modified Barth's Solution (MBS, pH 7.6). Embryos were staged according to the method of Nieuwkoop (*23*).

Generation of Xenopus Cav-1 and -2 Hybridization Probes. Regions with high levels of homology were determined by alignment of the known murine, human, and pufferfish sequences. Degenerate oligonucleotides (≤5-fold degeneracy) were designed (Cav-1, 5′-CARGGSAACATYTACAARCC-3′ (sense) and 5′-GGYACMACIGCCCAGATRTG-3′ (antisense); Cav-2, 5′-ATGGGKCTGGARAMSGARAA-3′ (sense) and 5′-TCYGTYACRSWYTTCCA-3′ (antisense), where R is A or G, Y is C or T, S is G or C, W is A or T, K is G or T, M is A or C, and I is inosine) and used in RT-PCRs of stage 30 *Xenopus* RNA, which yielded predicted PCR products of 335 and 413 bp, respectively. Re-amplification using dNTPs containing digoxigenin-dUTP (Roche Biochemicals) was used to generate the hybridization probes.

Library Screening and cDNA Cloning of Caveolins-1 and -2. A λ-phage cDNA library (*Xenopus* stage 30 embryo, Lambda-ZAP II #936652, Stratagene, Inc.) was used for screening. Primary library screening was conducted by plating phage at a density of 50 000 pfu/plate on ten 150 mm agar plates, lifting plaques using Hybond-N membranes (Amershan Pharmacia Biotech), and hybridizing with digoxigenin-labeled Cav-1- or Cav-2-specific probes (generated as described above). All further hybridization and detection steps were performed using the DIG nucleic acid detection kit (Roche Biochemicals), as per the manufacturer's instructions. Positive plaques were scored using a small Pasteur pipet and rehydrated in Luria broth containing 10 mM $MgSO_4$ and 10 mM maltose. Secondary and, sometimes when necessary, tertiary screens were performed exactly as described above, except using 10 cm agar plates. Ten positive phagemids from each of the Cav-1 and -2 screens were subjected to in vivo excision, as per the manufacturer's instructions (Stratagene, Inc.), yielding pBluescript SK(−) bacterial expression vectors containing the desired clones. Each vector was sequenced using the T7 and T3 primers, and possible alignments were made via DNA Sequencher software. Thus, open reading frames (ORFs) and protein sequences of the *Xenopus* Cav-1 and -2 cDNAs were deduced.

cDNA Cloning of Caveolin-3. As the cloning of the Cav-1 and -2 cDNA was ongoing, several ESTs were deposited in GenBank databases that were highly homologous to mammalian caveolin-3. Two ESTs (accession numbers AW766709 and AW767386) that are highly homologous to mammalian Cav-3 were then purchased from Research Genetics. Analysis and sequencing of both clones revealed that they are identical cDNAs, albeit spanning different portions of the ORF. Primers were designed to the extreme 5′ and 3′ ends of the ORF, used in RT-PCRs of stage 30 *Xenopus* RNA to obtain the entire cDNA, and subcloned in the pBluescript SK(−) vector. Sequences were determined using T7 and T3 primers.

Northern Blot Analysis of RNA from Embryos and Tissues. Total RNA was extracted from 100 mg of embryos or whole organs using the Trizol reagent (Gibco), as per the manufacturer's instructions. Twenty micrograms of total RNA for each sample was separated using a 1.0% agarose gel under RNase-free conditions and transferred to nitrocellulose. Cav-1, -2, and -3 probes were labeled with [^{32}P]dCTP using a random-priming kit (Stratagene, Inc.), and the filters were hybridized using the ExpressHyb solution (Clontech). The 28S and 18S RNAs (used as a control for equal RNA loading) were visualized by ethidium bromide staining of the agarose gel.

Immunoblot Analysis of Tissues. Freshly dissected tissue samples were washed thoroughly with PBS and either snap-frozen in liquid N_2 or immediately homogenized with lysis buffer [10 mM Tris (pH 7.5), 50 mM NaCl, 1% Triton X-100, and 60 mM octyl glucoside] containing protease

inhibitors (Roche Biochemicals). Protein concentrations were quantified using the BCA reagent (Pierce), and the volume required for 10 μg of protein was determined. Samples were separated by SDS−PAGE (12.5% acrylamide) and transferred to nitrocellulose. The nitrocellulose membranes were stained with Ponceau S (to visualize protein bands) followed by immunoblot analysis. All subsequent wash buffers contained 10 mM Tris (pH 8.0), 150 mM NaCl, and 0.05% Tween-20, which was supplemented with 1% bovine serum albumin (BSA) and 2% nonfat dry milk (Carnation) for the blocking solution and 1% BSA for the antibody diluent. Primary antibodies were used at a 1:500 dilution. Horseradish peroxidase-conjugated secondary antibodies (1:5000 dilution, Pierce) were used to visualize bound primary antibodies with the Supersignal chemiluminescence substrate (Pierce). Antibodies and their sources were as follows: anti-caveolin-1 mAb 2297, anti-caveolin-2 mAb 65, and anti-caveolin-3 mAb 26 (*10*, *24*, *25*) (gifts from R. Campos-Gonzalez, BD Transduction Laboratories, Inc.) and anti-caveolin-1 pAb N-20 (Santa Cruz Biotechnology).

Whole Mount in Situ Hybridization. Albino embryos were fixed overnight in MEMFA at 4 °C and rehydrated in 100% ethanol. Antisense probes for *Xenopus* Cav-1, -2, and -3 (encompassing the full cDNA sequences and incorporating digoxigenin-UTP) were prepared by in vitro transcription and used to analyze transcript patterns, as described previously (*26*). BM-purple AP substrate (Boehringer Mannheim) replaced NBT/BCIP as a substrate for color development.

Histology. Embryos were fixed in MEMFA containing 0.025% glutaraldehyde for 30 min at room temperature. The samples were rehydrated through a graded series of ethanol, cleared in xylene for 30 min, and embedded in Paraplast (Oxford) at 60 °C. Sections were cut at a thickness of 14 μm and placed on glass slides. After being deparaffinized in xylene twice for 2 min, sections were mounted with glass cover slips using Permount (Fisher Scientific).

RESULTS

Identification and Molecular Cloning of the cDNAs Encoding X. laevis Cav-1, -2, and -3. When this study was initiated, a search of *Xenopus*-expressed sequence tags (ESTs) and genomic databases revealed no sequences that were homologous to any of the known caveolin sequences. We thus decided to sequentially screen an embryonic (stage 30) *Xenopus* λ-phage cDNA library for the caveolin genes. For this purpose, we isolated probes by performing RT-PCRs on stage 30 RNA, using degenerate PCR primers derived from regions with high levels of conservation among previously known caveolins (see Experimental Procedures for a detailed description). The *Xenopus* caveolin-1 (xCav-1) and caveolin-2 (xCav-2) cDNAs were cloned in this fashion and the sequences (Figure 1) deposited in GenBank (accession numbers AF455042 and AF455043).

Later database searches revealed two ESTs (accession numbers AW766709 and AW767386) that were highly homologous to mammalian Cav-3. Analysis and sequencing of both clones revealed that together, they contain an ORF encoding a protein homologous to caveolin-3. A fragment encompassing the full ORF was isolated by RT-PCR (xCav-3), and the sequence (Figure 1) has also been deposited in GenBank (accession number AF455044).

The sequences of caveolin cDNAs have been reported previously for several species, mainly in the mammalian class. Cav-1 sequences are known for human, murine, bovine, canine, chicken, fugu, and the nematode *C. elegans* (*14*, *15*, *27*, *28*), Cav-2 sequences for human, murine, fugu, and *C. elegans* (*7*, *29*), and Cav-3 sequences for human and murine (*8*). A previous alignment of these sequences has revealed several interesting features. A stretch of eight amino acids (FEDVIAEP) is highly conserved and is now termed the "caveolin signature motif". Other highly conserved stretches are the *oligomerization domain* (a region shown to be involved in the oligomerization of the caveolins into complexes of ∼14−16 monomers) (*30*), the *scaffolding domain* (a subregion of the oligomerization domain implicated in the functional interaction with signaling molecules) (*13*, *31*), and a highly hydrophobic *membrane-spanning domain* (a region shown to be necessary for the "hairpin" insertion of the caveolins into the plasma membrane) (*32*). Alignments of the xCav-1, xCav-2, and xCav-3 predicted protein sequences with the known protein sequences of each caveolin are shown in Figure 2 (panels A−C, respectively). We deliberately omitted the *C. elegans* Cav-1 and -2 sequences as they are significantly more divergent compared to the vertebrate sequences.

xCav-1 is ∼80% identical to the human Cav-1 sequence, with most of the divergence occurring at the amino terminus (Figure 2A). The bulk of the protein containing the oligomerization (including the caveolin signature motif), scaffolding, and membrane-spanning domains is highly homologous (∼95% identical). However, the xCav-1 protein is longer than all other Cav-1 sequences by 39 amino acids, mostly due the presence of nonconserved residues at the N-terminus. Despite this N-terminal divergence, the known site of caveolin-1 tyrosine phosphorylation by c-Src (Y14 in human Cav-1) is highly conserved (see the arrow in Figure 2A). This localized divergence is most likely explained by the genomic organization of the Cav-1 locus. Mammalian Cav-1 is composed of three exons with the bulk of the protein encoded by exons 2 and 3, while the first exon encodes only 10 amino acids (*33*, *34*). Interestingly, the region with the highest level of homology in xCav-1 starts at the 11th amino acid (Figure 2A), indicating that the primary divergence is restricted to exon 1. In this regard, the *C. elegans* Cav-1 protein is also elongated and divergent at its extreme N-terminal region (*15*).

xCav-2 is ∼64% identical to the human Cav-2 sequence, and as with xCav-1, most of the divergence occurs at the N-terminus. Of all the caveolins, the least is known about the structure and function of Cav-2. Although it contains regions that are somewhat identical to both Cav-1 and -3 (i.e., the oligomerization and scaffolding domains), Cav-2 is not able to oligomerize on its own and its scaffolding domain does not behave like the other caveolins (*7*, *35*). In fact, it requires the presence of Cav-1 to both hetero-oligomerize and localize to caveolae (*12*, *36*, *37*). Two amino acid stretches on the flanking ends of its membrane-spanning domain mediate the hetero-oligomerization with Cav-1 (*29*). As delineated in Figure 2B, xCav-2 is highly conserved in all these regions.

xCav-3 is ∼45% identical to the human Cav-3 sequence (Figure 2C). At first glance, this is surprising in light of the high level of identity between xCav-1 and the other mam-

Xenopus Caveolin-1

```
    ATG GGG ATC ATT CTC AAC GCA GCT TCG TGT CAC AGC TCT CAC CCT ATT CCC ATC TAT GGT GGC ACT GCT GCG CTA ACT GTC ACT TGT CTT TTC TCT CCT TCG CTC TCT CCT TGT CCG TCC
  1 M   G   I   I   L   N   A   A   S   C   H   S   S   H   P   I   P   I   Y   G   G   T   A   A   L   T   V   T   C   L   F   S   P   S   L   S   P   C   P   S
    CGC TCC CTC CAG GGT GTT CTC TAC ACC ACG CCG GTC ATC AGA GAG CAC GGC AAC ATC TAC AAA CCC AAC AAC AAG ACC ATG GCA GAT GAT TTC CTG ACT GAG ACT GAA GTC CGC GAC TCG
 41 R   S   L   Q   G   V   L   Y   T   T   P   V   I   R   E   H   G   N   I   Y   K   P   N   N   K   T   M   A   D   D   F   L   T   E   T   E   V   R   D   S
    CAC ACC AAG GAG ATC GAT CTG GTC AAC AGG GAC CCC AAG CAC CTC AAT GAC GAT GTG GTT AAG ATC GAT TTT GAA GAC GTG ATT GCT GAA CCA GAT GGG ACA CAT AGC TTC GAT GGC ATC
 81 H   T   K   E   I   D   L   V   N   R   D   P   K   H   L   N   D   D   V   V   K   I   D   F   E   D   V   I   A   E   P   D   G   T   H   S   F   D   G   I
    TGG AAA ACA AGC TTC ACT ACA TTC ACT GTC ACA AAG TAC TGG TTC TAT CGG CTG CTG TCT GCT ATC TTT GGC ATC CCA TTG TCA CTT ATC TGG GGC ATC TTC TTT GCC ATC CTC TCC TTC
121 W   K   T   S   F   T   T   F   T   V   T   K   Y   W   F   Y   R   L   L   S   A   I   F   G   I   P   L   S   L   I   W   G   I   F   F   A   I   L   S   F
    CTG CAC ATC TGG GCA GTG GTG CCA TGC ATA CGA AGC TAC TTG ATT GAG ATT CAA TTT CTT AGC CGG GTC TAT TCC ATC GGT GTC CAC ACC TTA TTT GAC CCG TGG TTT GAA GCC ATG GGC
161 L   H   I   W   A   V   V   P   C   I   R   S   Y   L   I   E   I   Q   F   L   S   R   V   Y   S   I   G   V   H   T   L   F   D   P   W   F   E   A   M   G
    AAA ATG CTC AGT TTT ATT AAG ATT TCC TTA CCG CAA AGA AGT GTA GGT GAC TAT TAC TGA
201 K   M   L   S   F   I   K   I   S   L   P   Q   R   S   V   G   D   Y   Y   *
```

Xenopus Caveolin-2

```
    ATG GGC CTC GAG AAG GAG ACG TTA GAT GCC CGC ATT TTT ATG GAC GAA GAT GAA CTG AAT CAC AGC ACT GTC CCC ATG CTC ACT GAA AAG ACA TTC GAC AAC AGC CCC GAC CGT GAT CCC
  1 M   G   L   E   K   E   T   L   D   A   R   I   F   M   D   E   D   E   L   N   H   S   T   V   P   M   L   T   E   K   T   F   D   N   S   P   D   R   D   P
    AAG AGG CTG AAC TCC CAC CTG AAG ATA GAG TTT GAG GAT GTG ATC GGA GAG CCA GAT ACA ACT CAC AGC TTC GAC AGG GTC TGG GTG TGC AGC ACA GCT CTG TTT GAA ATC AGC AAA TAC
 41 K   R   L   N   S   H   L   K   I   E   F   E   D   V   I   G   E   P   D   T   T   H   S   F   D   R   V   W   V   C   S   T   A   L   F   E   I   S   K   Y
    CTG ATC TAC AAG GTC CTC ACT GTC CTA CTT GCT GTG CCG CTG GCA TTT GTA ATG GGA ATA CTA TTT GCA GTG CTC AGC TGT CTA CAC ATT TGG ATT ATG ATG CCT TTC GCG AAG ACC TGT
 81 L   I   Y   K   V   L   T   V   L   L   A   V   P   L   A   F   V   M   G   I   L   F   A   V   L   S   C   L   H   I   W   I   M   M   P   F   A   K   T   C
    ATG ATG ATT TTG CCT TCT GTA CAG AAG ATA TGG AAG GGC GTG ACA GAT AGC TTT ATT GCT CCC TTA TTT GCA AGC ATG GGA CGG TGT ATG TCT AGC ATT AAC ATT CAG TTG GAT CGG GAT
121 M   M   I   L   P   S   V   Q   K   I   W   K   G   V   T   D   S   F   I   A   P   L   F   A   S   M   G   R   C   M   S   S   I   N   I   Q   L   D   R   D
    TAA
161 *
```

Xenopus Caveolin-3

```
    ATG GCT GAG CCC AAA TCC ATC CCC AAT GAG CCC ATG CCT CTG GAC ATG GAC AAC CGG GAC CCT AAT AAC TTG AAT GAT CAT GTC AGG GTG CTG TTT GAG GAT GCC TTT GGG GAG CCA GAA
  1 M   A   E   P   K   S   I   P   N   E   P   M   P   L   D   M   D   N   R   D   P   N   N   L   N   D   H   V   R   V   L   F   E   D   A   F   G   E   P   E
    GGA TCT CAC AGC ATT CCG GGA GTG TGG AGC ATG TCC TAC AAA ACC TTC AAC GGG GTG AAG AAC TGC TGC TAC ATT GTG CTG TCG GTG CTG TGC GGG TGC CCC CTG GCC TTC TGC TGG GCG
 41 G   S   H   S   I   P   G   V   W   S   M   S   Y   K   T   F   N   G   V   K   N   C   C   Y   I   V   L   S   V   L   C   G   C   P   L   A   F   C   W   A
    CTG GAG TTT GCC TGT GTA CAG TGC TGC CAT ATC TGG ATG GTG GGC CCT TGT ATT CAC ATC TGG AAG ATA AAT GTG TCC TGT ATG AAG ATG TTC TAT AGC TCC TGT GTG CAC TGT CTG TGT
 81 L   E   F   A   C   V   Q   C   C   H   I   W   M   V   G   P   C   I   H   I   W   K   I   N   V   S   C   M   K   M   F   Y   S   S   C   V   H   C   L   C
    GAC CCA TGC TGG GAG GCG TGT GGC TTG TGC TTA AGT CTC ATT CGG GTG CAG AAT AAG AAC GGA TAG
121 D   P   C   W   E   A   C   G   L   C   L   S   L   I   R   V   Q   N   K   N   G   *
```

FIGURE 1: cDNA sequences and deduced protein sequences of the caveolin gene family in *X. laevis*. Numbers at the left indicate amino acid positions. Termination codons are denoted with asterisks. The predicted xCav-1 protein is 219 amino acids long, xCav-2 is 160 amino acids long, and xCav-3 is 141 amino acids long.

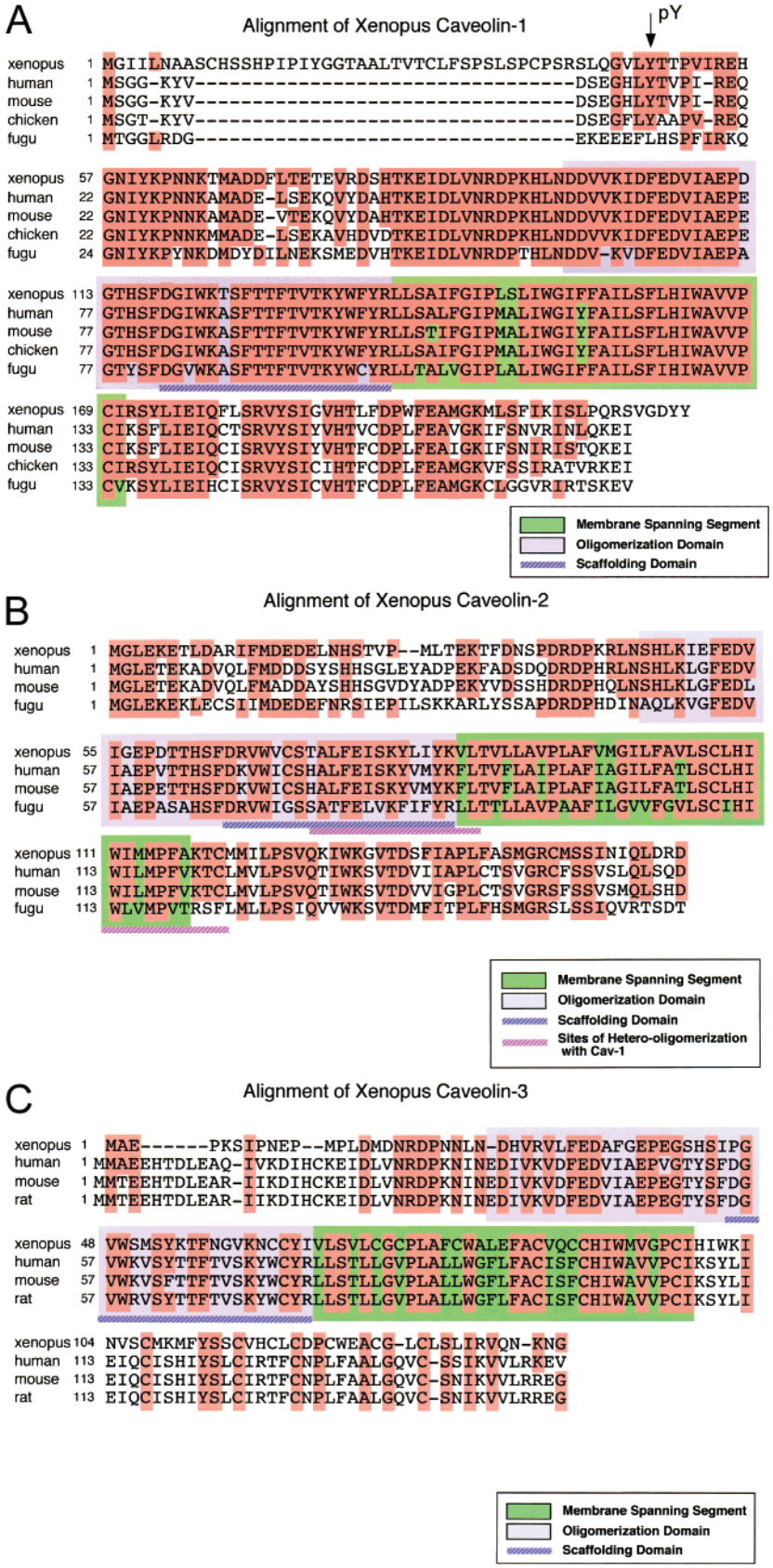

FIGURE 2: Alignment of the *Xenopus* caveolin gene family with the protein sequences of currently known caveolin genes. Residues identical to the *Xenopus* caveolins are highlighted in pink. Residues that span the oligomerization and membrane-spanning domains of the caveolins are demarcated by blue and green backgrounds, respectively. The scaffolding domain, which is a subset of the oligomerization domain, is underlined with a cross-hatched blue line. (A) Cav-1. Alignment of *Xenopus* caveolin-1 with the human, mouse, chicken, and fugu caveolin-1 sequences. Note the long amino-terminal extension present in xCav-1 but not in the other caveolin-1 proteins. An arrow points at the conserved site of c-Src-mediated tyrosine phosphorylation. (B) Cav-2. Alignment of *Xenopus* caveolin-2 with the human, mouse, and fugu caveolin-2 sequences. As Cav-2 cannot homo-oligomerize, residues shown to be important for its hetero-oligomerization with Cav-1 are underlined with a cross-hatched violet line. (C) Cav-3. Alignment of *Xenopus* caveolin-3 with the human, mouse, and rat caveolin-3 sequences. Note that of all three *Xenopus* caveolins, xCav-3 is least similar to its mammalian counterparts.

malian Cav-1's. On the basis of the high degree of homology between mammalian Cav-1 and Cav-3 and the fact that there is only one homologous caveolin gene in *C. elegans*, it has previously been proposed that Cav-1 and -3 probably evolved from a common ancestor (*15*). However, until now, a nonmammalian Cav-3 gene has not been described. Although many residues in the membrane-spanning, oligomerization, and scaffolding domains are conserved, our finding of a relatively low level of identity between xCav-3 and the other mammalian Cav-3 proteins is intriguing. However, much like its mammalian homologue, xCav-3 is specifically expressed in muscle tissues (see Figure 3A below). Therefore, despite the lack of homology, the function of xCav-3 may be highly conserved from amphibians to mammals.

Tissue-Specific Expression of Xenopus Caveolins in the Adult Frog. Thus far, the most thorough analysis of tissue-specific expression of the caveolins has been conducted in the mouse (*7*−*9*). From these reports and other more restricted studies on specific cells and tissues, it appears that all three proteins are present at their highest levels in terminally differentiated cells. Interestingly, the expression patterns of caveolin-1 and -2 are largely distinct from that of caveolin-3; whereas adipocytes, endothelial cells, pneumocytes, and fibroblasts have the highest levels of caveolin-1 and -2, caveolin-3 expression is limited to muscle cell types (i.e., cardiac and skeletal muscle cells) (*7*−*9*). Certain cell types (namely, smooth muscle) have expression of all three proteins possibly due to the hybrid fibroblastic/myocytic nature of this cell.

We next assessed the tissue distribution of *Xenopus* caveolins by Northern blot analysis, using the isolated cDNAs as probes (Figure 3A). xCav-1 and Cav-2 expression is to a large extent overlapping, and levels are highest in the lung and fat body (most likely due to the enrichment in endothelial cells or pneumocytes and adipocytes, respectively), with lower transcript levels also observed in the skin, stomach, and intestine. The xCav-3 transcript pattern is quite distinct from those of the other two caveolins and is mostly limited to the heart and skeletal muscle tissues. Therefore, the expression patterns of caveolin-1, -2, and -3 in adult tissues of a nonmammalian vertebrate are almost identical to that previously reported for mammals.

Several highly specific commercially available antibodies have been generated against all three mammalian caveolin family members. These include a monoclonal antibody (mAb) directed against residues 61−71 of chicken Cav-1, a polyclonal Ab against residues 1−20 of human Cav-1, a mAb against residues 79−88 of mouse Cav-2, and a mAb against residues 3−24 of rat Cav-3 (see also Experimental Procedures). Given the highly conserved domain structure of some of the caveolins (Figure 2), we considered whether these antibodies might cross-react with *Xenopus* caveolins. Immunoblot analysis of protein lysates from the same panel of tissues used in Figure 3A shows that only the mAb directed against Cav-1 was able to detect *Xenopus* proteins (Figure 3B; data not shown for the negative immunoblots). In corroboration with the Northern blot analysis, this anti-Cav-1 mAb detected an ~25 kDa protein in primarily the fat body and lungs, with lower levels of expression in the skin, stomach, intestines, and heart. The lack of protein detection with the other three antibodies is not entirely surprising since all the epitopes recognized by the other antibodies are to regions of the proteins that are not entirely conserved in the *Xenopus* caveolins.

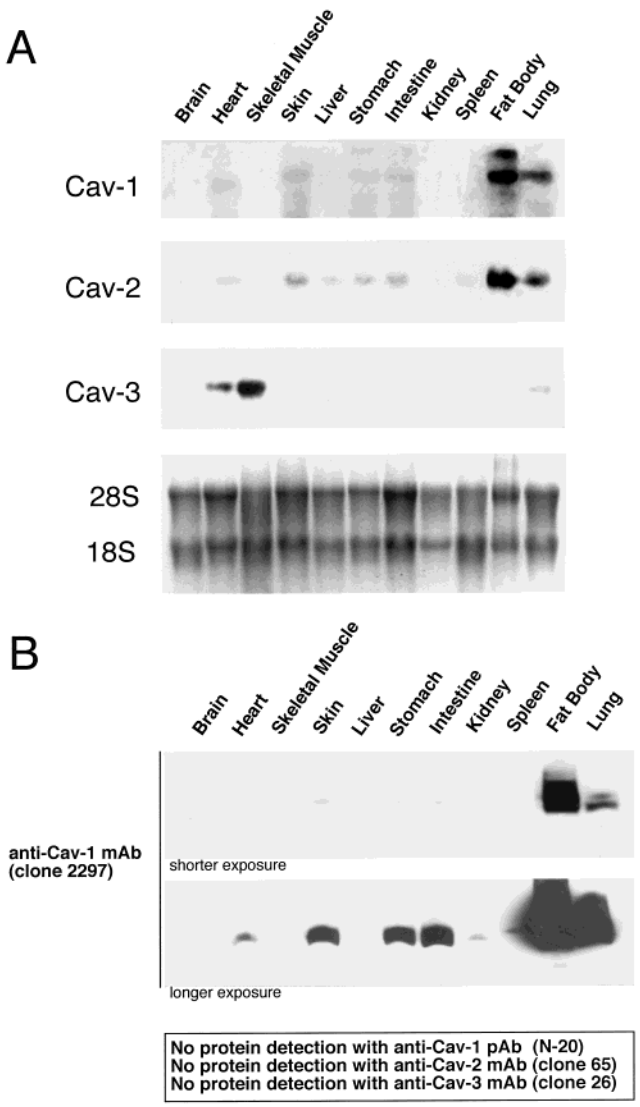

FIGURE 3: Northern blot and Western blot analyses of the tissue-specific distribution of *Xenopus* caveolins in the adult frog. (A) Northern blot analysis. Total RNA was extracted from the indicated tissues, and 20 μg was subjected to Northern blot analysis using the randomly primed xCav-1, xCav-2, and xCav-3 cDNAs. Equal loading was assessed by ethidium bromide staining of the gel (revealing the prominent 28S and 18S rRNA bands). (B) Western blot analysis. Protein lysates from the indicated tissues were prepared, and 20 μg was subjected to SDS−PAGE/immunoblot analysis using antimammalian caveolin antibodies, as follows: anti-Cav-1 mAb (clone 2297), anti-Cav-1 pAb (designated N-20), anti-Cav-2 mAb (clone 65), and anti-Cav-3 mAb (clone 26). Note that immunoreactive bands were detected only with the anti-Cav-1 mAb (clone 2297), thereby revealing an expression pattern that is consistent with the Northern blotting experiments shown in panel A.

Temporal and Spatial Expression of the Xenopus Caveolins during Embryogenesis. We next sought to determine the patterns of expression for the *Xenopus* caveolins at various stages of embryogenesis. First, we conducted Northern blot analysis on RNA derived from a series of *Xenopus* embryonic stages [stage 0 (unfertilized egg) to stage 46 (tadpole)] (Figure 4A,B). At this level of sensitivity, xCav-1, -2, and -3 transcripts are first detectable at stage 33, and their levels increase steadily thereafter. The simultaneous increase in the

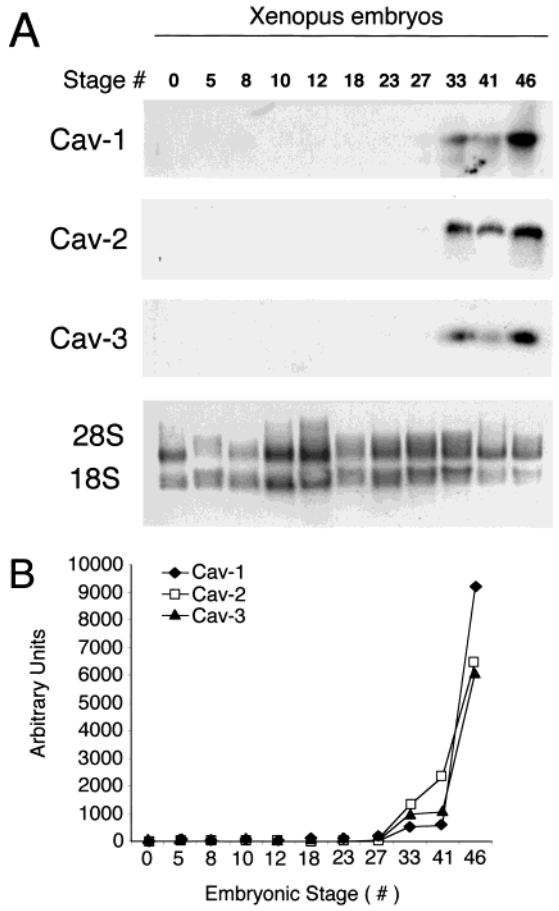

FIGURE 4: Northern blot analysis of the embryonic expression of the *Xenopus* caveolins, spanning stages 0 to 46. (A) Total RNA was extracted from the indicated embryonic stages, and 20 μg was subjected to Northern blot analysis using the randomly primed xCav-1, xCav-2, and xCav-3 cDNAs. Equal loading was assessed by ethidium bromide staining of the gel, revealing the prominent 28S and 18S rRNA bands. (B) Northern blot data were analyzed by densitometry using Imagequant software and are presented graphically. xCav-1, -2, and -3 expression levels were normalized to the amount of 28S or 18S rRNA in a given lane.

levels of all three caveolins at these later stages is consistent with their accumulation during tissue differentiation.

To determine if there is spatial regulation of caveolin expression during very early embryogenesis, we also conducted in situ hybridization on a series of embryos during early development. Figure 5 shows representative whole mounts and transverse sections. xCav-1 (Figure 5A) and xCav-2 (Figure 5B) show similar spatial and temporal changes in their expression patterns. Maternal and/or zygotic transcripts of Cav-1 and -2 are present with no discrete localization until neural stages [panels i and ii of part A and panel i (left) of part B]. At the end of neurulation [panel i (right) of part B], the transcript levels decline in a wide area of the trunk, excluding dorsal axial mesoderm/ectoderm tissues. At early tailbud stage, xCav-1 (panels iv−vi of part A) as well as xCav-2 (panel ii of part B) localizes in dorsal tissues, including the notochord and somites, the cement gland, eye vesicle, and posterior tailbud. A transverse section at the tailbud stage (panel vii of part B) reveals xCav-2 transcripts in the notochord and the neighboring somite tissues, and lightly in neural tube; identical results were also obtained for xCav-1 (data not shown). At the tadpole stages, cells expressing Cav-1 and -2 are found more specifically in notochord, somites, branchial arch, cement gland, and olfactory placode. The failure to detect transcripts at these earlier stages by Northern blotting presumably reflects the lower level of sensitivity for this assay.

In contrast to xCav-1 and -2, maternal xCav-3 transcripts are absent throughout the cleavage stages (data not shown). During the early neurulation stages, zygotic transcripts of Cav-3 appear in non-neural ectoderm, in a strikingly spaced pattern (Figure 6). The Cav-3 positive cells surround the entire epidermal ectoderm and are distinctly missing along the neural plate and in cement gland (see the arrows in panels iv and vii of Figure 6). In the transverse sections shown in Figure 6 (stages 23−37), xCav-3-expressing cells are distributed at intervals in the outer layer of developing double-layered epidermis in tailbuds and tadpoles. This pattern is remarkably similar to that described previously for α-tubulin (*38*).

DISCUSSION

Here, we have described the primary structure of the three *Xenopus* caveolin homologues (termed xCav-1, xCav-2, and xCav-3) and established their expression patterns in the developing embryo and adult frog. We found that xCav-1 and xCav-2 have a large degree of identity with the previously known caveolins and high levels of homology in domains implicated in caveolin structure and function. More surprising was the relatively low level of homology between xCav-3 and Cav-3 from the mammalian species (~45% identical), particularly in light of the much higher level of conservation between xCav-1 and the other Cav-1's. On the basis of the high level of homology between mammalian Cav-1 and Cav-3 and the fact that there is only one homologous caveolin gene in *C. elegans*, it had been proposed that Cav-1 and -3 probably evolved from a common ancestor (*15*). However, until now, a nonmammalian Cav-3 gene has not been described. Although many residues in the membrane-spanning, oligomerization, and scaffolding domains are conserved, our finding of a relatively low level of identity between xCav-3 and the other Cav-3 proteins may not be consistent with this previous notion.

Despite the varying levels of homology between the *Xenopus* caveolins, they are clearly present in the same adult tissues as the mammalian caveolins. xCav-1 and xCav-2 show overlapping expression predominantly in the fat body and lungs, while xCav-3 was expressed in heart and skeletal muscle tissue. The identical tissue distribution of the caveolin family members from amphibians to mammals cleary emphasizes the conserved functional roles of the different caveolin genes.

Using Northern blot analysis, we examined the stage-specific expression of xCav-1, -2, and -3 during *Xenopus* embryogenesis. The upregulation of the caveolin genes during the latter stages of embryogenesis is consistent with the development of adipose and muscle tissue. Recently, Chan et al. characterized the stage and tissue expression of *fatvg*, the frog homologue of the adipose differentiation-related protein (ADRP) (*39*). Interestingly, in stage 40 embryos, *fatvg* mRNA was detected in parallel stripes along the endodermal mass, which would later develop into the fat bodies (*39*). Consistent with these findings, xCav-1 and -2 are markedly upregulated after stage 41, coincident with

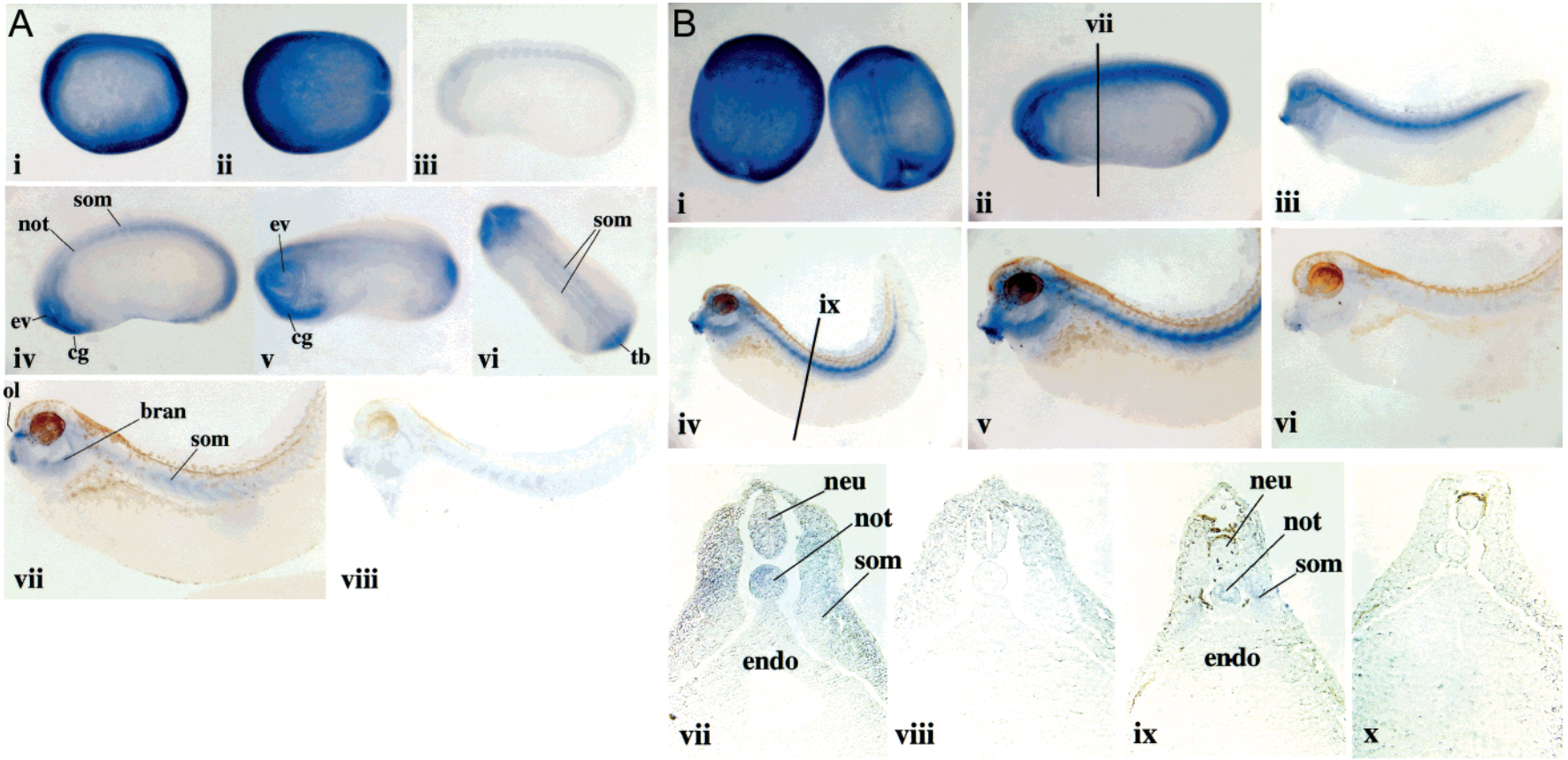

FIGURE 5: Analysis of the embryonic expression patterns of *Xenopus* Cav-1 and Cav-2 via in situ hybridization. (A) xCav-1 expression at neurula stage 17 [lateral (i) and dorsal (ii) views], tailbud stage 22 [lateral (iv), ventro-lateral (v), and dorsal (vi) views], and tadpole stage 37 (vii). Panels iii and viii show representative embryos hybridized with a control sense probe, as a negative control. Abbreviations: ev, eye vesicle; cg, cement gland; not, notochord; som, somite; ol, olfactory placode; bran, branchial arch; tb, tailbud. (B) xCav-2 expression at neurula stages 17 (i, left) and 19 (i, right), tailbud stages 22 (ii and vii) and 26 (iii), and tadpole stage 37 (iv, v, and ix). Panels vi, viii, and x show representative embryos hybridized with a control sense probe, as a negative control. Panels vii−x are tissue sections. Abbreviations: not, notochord; som, somite; neu, neural tube; endo, endoderm. Representative stages of the whole mounts and transverse sections are shown, where xCav-1 (A) and xCav-2 (B) exhibit similar spatial and temporal changes in their expression patterns. Maternal and/or zygotic transcripts of Cav-1 and -2 are present with no discrete localization until neural stages [panels i and ii of part A and panel i (left) of part B]. At the end of neurulation [panel i (right) of part B], the transcript levels decline in a wide area of the trunk, excluding dorsal axial mesoderm/ectoderm tissues. At early tailbud stage, xCav-1 (panels iv−vi of part A) as well as xCav-2 (panel ii of part B) localizes in dorsal tissues, including the notochord and somites, the cement gland, eye vesicle, and posterior tailbud. A transverse section at the tailbud stage (panel vii of part B) reveals xCav-2 transcripts in the notochord and the neighboring somite tissues, and lightly in neural tube; identical results were also obtained for xCav-1 (not shown). At the tadpole stages, cells expressing Cav-1 and -2 are found more specifically in notochord, somites, branchial arch, cement gland, and olfactory placode. The failure to detect transcripts at these earlier stages by Northern blotting presumably reflects the level of sensitivity for the assay.

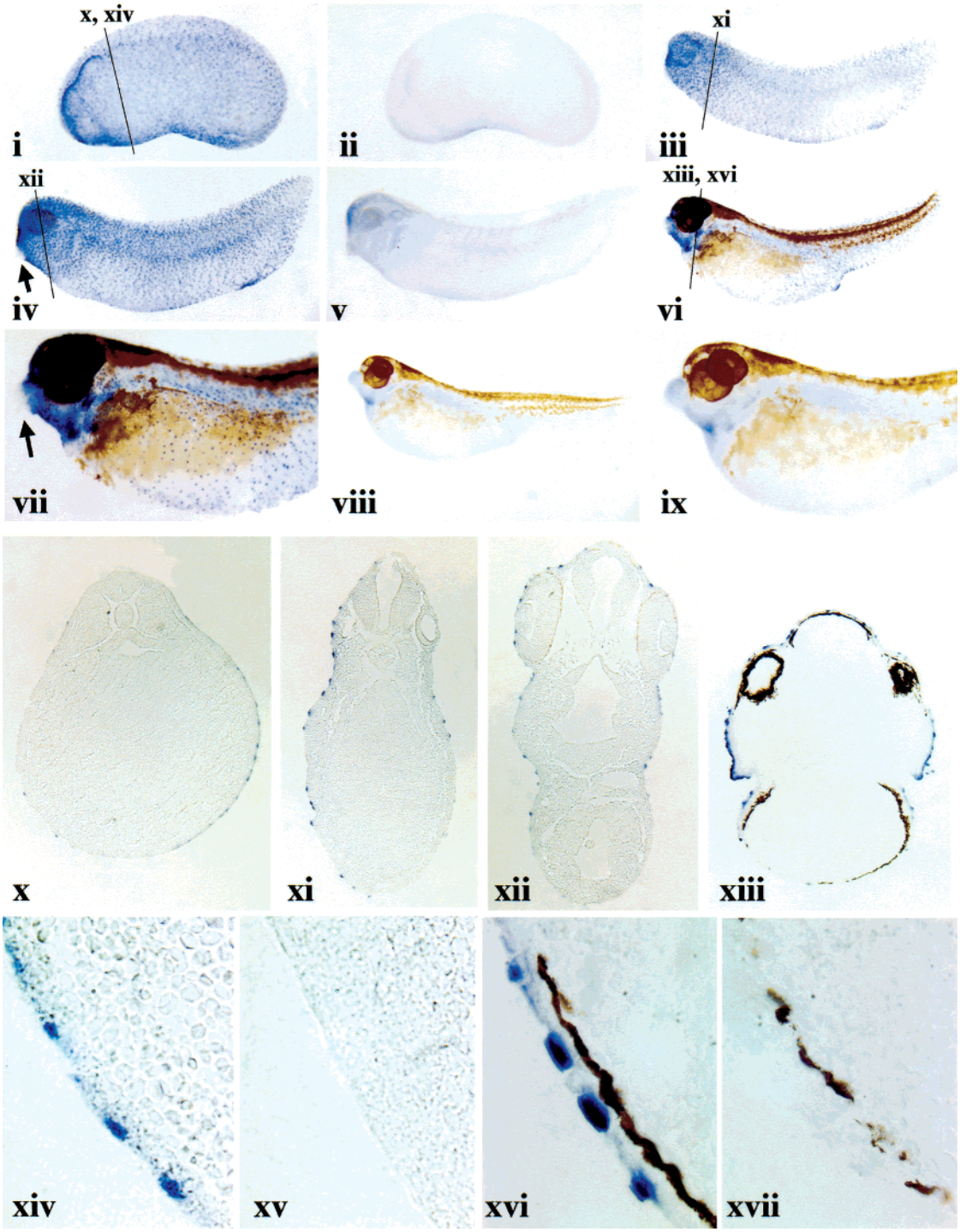

FIGURE 6: Analysis of the embryonic expression patterns of *Xenopus* Cav-3 via in situ hybridization. The punctate xCav-3 expression patterns at tailbud stages 22 and 23 (i, x, and xiv), 26 (iii and xi), and 28 (iv and xii) and at tadpole stage 37 (vi, vii, xiii, and xvi) are shown. Panels ii, v, viii, ix, xv, and xvii show representative embryos hybridized with a control sense probe, as a negative control. Panels x−xvii are tissue sections. Note that during the early neurulation stages, zygotic transcripts of Cav-3 appear in non-neural ectoderm, in a strikingly spaced pattern. The Cav-3 positive cells surround the entire epidermal ectoderm and are distinctly missing along the neural plate and in cement gland (panels iv and vii; see the arrows). In the transverse sections shown, xCav-3-expressing cells are distributed at intervals in the outer layer of the developing double-layered epidermis in tailbuds and tadpoles.

primordial fat body development. The appearance of caveolin-3 at stage 33 is consistent with hypaxial muscle migration and ventral body wall myogenesis, which occurs during this embryonic stage (*40*).

The recent characterization of caveolin-deficient mice clearly demonstrates the importance and versatility of caveolins in the maintenance of normal tissue functioning, especially lung, adipose, and muscle tissues (*12*, *41*, *42*). Interestingly, caveolin-1-deficient mice exhibit a lean-body phenotype due to adipocyte abnormalities and display altered lipoprotein profiles (*43*). Therefore, the expression of xCav-1 in developing and mature fat bodies stresses the importance of Cav-1 in the regulation of lipid homeostasis by mammalian and amphibian fat pads. Caveolin-3, on the other hand, has been shown to be transiently associated with developing T-tubules and to play a role in the formation of

the T-tubule system in differentiating muscle cells (*44*). Also, Cav-3-deficient mice were shown to have structural abnormalities of the T-tubule system, being dilated and highly disorganized (*45*, *46*). Similar defects in T-tubule organization were observed in patients with LGMD-1C (*47*), a form of autosomal dominant limb girdle muscular dystropy seen in humans with dominant-negative mutations within the caveolin-3 gene [such as P104L or ΔTFT(63−65)] (*48*−*50*). Thus, the expression of xCav-3 early in muscle differentiation suggests that it may play a similar role in the proper skeletal muscle development of *Xenopus*.

We also presented the first detailed analysis of caveolin expression during embryonic development using in situ hybridization techniques. The expression of xCav-1 and xCav-2 in the notochord is interesting given the important role this tissue has as a signaling center, and the central function proposed for caveolins in regulating various signal transduction pathways. Interestingly, the peripherally localized punctate staining pattern seen for xCav-3 in embryos is highly reminiscent of the emergence of a population of evenly spaced ciliated cells in the skin of the developing embryo (*51*). Although the function of these cells in not yet known, the coordinated movements of their cilia likely act to move the surrounding mucous and fluid layers enabling the exchange of nutrients and oxygen. Recently, a report showed that the differentiation, migration, and eventual spatial patterning of these ciliated cells are regulated by the Notch signaling pathway (*38*). If the developmental expression of xCav-3 is indeed coincident with these cells, the current evidence supporting a role for the caveolins in the regulation of signal transduction may suggest a possible connection between the caveolins and Notch signaling. Future studies will have to assess the functional significance of this spatial and temporal localization.

X. laevis has served as an important model organism in the field of developmental biology for many years. Some of the obvious advantages of this experimental system include its relative rapidity in morphogenesis from zygote to tadpole, and the relative ease with which such changes can be observed in vitro. Furthermore, the *Xenopus* oocyte is widely used as a transcription and translation system for the ectopic expression of genes, a condition useful for both biochemical and functional studies. Thus, this report of the identification and expression of the three *Xenopus* caveolins will be extremely useful in several respects. Most importantly, it provides a new model system for the analysis of the caveolins and caveolae during development and beyond.

ACKNOWLEDGMENT

We thank Dr. Roberto Campos-Gonzalez (BD Transduction Laboratories) for donating mAbs directed against caveolin-1, caveolin-2, and caveolin-3.

REFERENCES

1. Palade, G. E. (1953) *J. Appl. Phys. 24*, 1424−1436.
2. Yamada, E. (1955) *J. Biophys. Biochem. Cytol. 1*, 445−458.
3. Simons, K., and Toomre, D. (2000) *Nat. Rev. Mol. Cell Biol. 1* (1), 31−39.
4. Galbiati, F., Razani, B., and Lisanti, M. P. (2001) *Cell 106* (4), 403−411.
5. Glenney, J. R., Jr., and Zokas, L. (1989) *J. Cell Biol. 108* (6), 2401−2408.
6. Rothberg, K. G., Heuser, J. E., Donzell, W. C., Ying, Y. S., Glenney, J. R., and Anderson, R. G. (1992) *Cell 68* (4), 673−682.
7. Scherer, P. E., Okamoto, T., Chun, M., Nishimoto, I., Lodish, H. F., and Lisanti, M. P. (1996) *Proc. Natl. Acad. Sci. U.S.A. 93*, 131−135.
8. Tang, Z.-L., Scherer, P. E., Okamoto, T., Song, K., Chu, C., Kohtz, D. S., Nishimoto, I., Lodish, H. F., and Lisanti, M. P. (1996) *J. Biol. Chem. 271*, 2255−2261.
9. Scherer, P. E., Lisanti, M. P., Baldini, G., Sargiacomo, M., Corley-Mastick, C., and Lodish, H. F. (1994) *J. Cell Biol. 127*, 1233−1243.
10. Song, K. S., Scherer, P. E., Tang, Z.-L., Okamoto, T., Li, S., Chafel, M., Chu, C., Kohtz, D. S., and Lisanti, M. P. (1996) *J. Biol. Chem. 271*, 15160−15165.
11. Fra, A. M., Williamson, E., Simons, K., and Parton, R. G. (1995) *Proc. Natl. Acad. Sci. U.S.A. 92*, 8655−8659.
12. Razani, B., Engelman, J. A., Wang, X. B., Schubert, W., Zhang, X. L., Marks, C. B., Macaluso, F., Russell, R. G., Li, M., Pestell, R. G., Di Vizio, D., Hou, H., Jr., Knietz, B., Lagaud, G., Christ, G. J., Edelmann, W., and Lisanti, M. P. (2001) *J. Biol. Chem. 276* (41), 38121−38138.
13. Razani, B., Schlegel, A., and Lisanti, M. P. (2000) *J. Cell Sci. 113* (Part 12), 2103−2109.
14. Tang, Z.-L., Scherer, P. E., and Lisanti, M. P. (1994) *Gene 147*, 299−300.
15. Tang, Z., Okamoto, T., Boontrakulpoontawee, P., Katada, T., Otsuka, A. J., and Lisanti, M. P. (1997) *J. Biol. Chem. 272*, 2437−2445.
16. Scheel, J., Srinivasan, J., Honnert, U., Henske, A., and Kurzchalia, T. V. (1999) *Nat. Cell Biol. 1* (2), 127−129.
17. Kordylewski, L. (1983) *Z. Mikrosk.-Anat. Forsch. 97* (4), 719−734.
18. Sawada, H., Ishikawa, H., and Yamada, E. (1978) *Tissue Cell 10* (1), 179−190.
19. Dulhunty, A. F., and Franzini-Armstrong, C. (1975) *J. Physiol. 250* (3), 513−539.
20. Latker, C. H., Shinowara, N. L., Miller, J. C., and Rapoport, S. I. (1987) *J. Comp. Neurol. 264* (3), 291−302.
21. Bundgaard, M., Hagman, P., and Crone, C. (1983) *Microvasc. Res. 25* (3), 358−368.
22. Levin, K. R., and Page, E. (1980) *Circ. Res. 46* (2), 244−255.
23. Nieuwkoop, P. D., and Faber, J. (1967) *Normal table of Xenopus laevis*, North-Holland Publishing Co., Amsterdam.
24. Scherer, P. E., Tang, Z.-L., Chun, M. C., Sargiacomo, M., Lodish, H. F., and Lisanti, M. P. (1995) *J. Biol. Chem. 270*, 16395−16401.
25. Scherer, P. E., Lewis, R. Y., Volonte, D., Engelman, J. A., Galbiati, F., Couet, J., Kohtz, D. S., van Donselaar, E., Peters, P., and Lisanti, M. P. (1997) *J. Biol. Chem. 272*, 29337−29346.
26. Brivanlou, A. H., and Harland, R. M. (1989) *Development 106* (3), 611−617.
27. Glenney, J. R., Jr., and Soppet, D. (1992) *Proc. Natl. Acad. Sci. U.S.A. 89* (21), 10517−10521.
28. Glenney, J. R. (1992) *FEBS Lett. 314*, 45−48.
29. Das, K., Lewis, R. Y., Scherer, P. E., and Lisanti, M. P. (1999) *J. Biol. Chem. 274*, 18721−18728.
30. Sargiacomo, M., Scherer, P. E., Tang, Z.-L., Kubler, E., Song, K. S., Sanders, M. C., and Lisanti, M. P. (1995) *Proc. Natl. Acad. Sci. U.S.A. 92*, 9407−9411.
31. Couet, J., Li., S., Okamoto, T., Ikezu, T., and Lisanti, M. P. (1997) *J. Biol. Chem. 272*, 6525−6533.
32. Monier, S., Parton, R. G., Vogel, F., Behlke, J., Henske, A., and Kurzchalia, T. (1995) *Mol. Biol. Cell 6*, 911−927.
33. Engelman, J. A., Zhang, X. L., Galbiati, F., and Lisanti, M. P. (1998) *FEBS Lett. 429*, 330−336.
34. Engelman, J. A., Zhang, X. L., and Lisanti, M. P. (1998) *FEBS Lett. 436*, 403−410.
35. Li, S., Galbiati, F., Volonte, D., Sargiacomo, M., Engelman, J. A., Das, K., Scherer, P. E., and Lisanti, M. P. (1998) *FEBS Lett. 434*, 127−134.
36. Parolini, I., Sargiacomo, M., Galbiati, F., Rizzo, G., Grignani, F., Engelman, J. A., Okamoto, T., Ikezu, T., Scherer, P. E., Mora, R., Rodriguez-Boulan, E., Peschle, C., and Lisanti, M. P. (1999) *J. Biol. Chem. 274* (36), 25718−25725.
37. Mora, R., Bonilha, V. L., Marmorstein, A., Scherer, P. E., Brown, D., Lisanti, M. P., and Rodriguez-Boulan, E. (1999) *J. Biol. Chem. 274* (36), 25708−25717.
38. Deblandre, G. A., Wettstein, D. A., Koyano-Nakagawa, N., and Kintner, C. (1999) *Development 126* (21), 4715−4728.
39. Chan, A. P., Kloc, M., Bilinski, S., and Etkin, L. D. (2001) *Mech. Dev. 100*, 137−140.

40. Martin, B. L., and Harland, R. M. (2001) *Dev. Biol. 239*, 270−280.
41. Razani, B., and Lisanti, M. P. (2001) *J. Clin. Invest. 108*, 1553−1561.
42. Drab, M., Verkade, P., Elger, M., Kasper, M., Lohn, M., Lauterbach, B., Menne, J., Lindschau, C., Mende, F., Luft, F. C., Schedl, A., Haller, H., and Kurzchalia, T. V. (2001) *Science 293* (5539), 2449−2452.
43. Razani, B., Combs, T. P., Wang, X. B., Frank, P. G., Park, D. S., Russell, R. G., Li, M., Tang, B., Jelicks, L. A., Scherer, P. E., and Lisanti, M. P. (2002) *J. Biol. Chem. 277*, 8635−8647.
44. Parton, R. G., Way, M., Zorzi, N., and Stang, E. (1997) *J. Cell Biol. 136*, 137−154.
45. Galbiati, F., Engelman, J. A., Volonte, D., Zhang, X. L., Minetti, C., Li, M., Hou, H., Kneitz, B., Edelmann, W., and Lisanti, M. P. (2001) *J. Biol. Chem. 19*, 19.
46. Galbiati, F., Razani, B., and Lisanti, M. P. (2001) *Trends Mol. Med. 7* (10), 435−441.
47. Minetti, C., Bado, M., Broda, P., Sotgia, F., Bruno, C., Galbiati, F., Volonte, D., Lucania, G., Pavan, A., Bonilla, E., Lisanti, M. P., and Cordone, G. (2002) *Am. J. Pathol. 160*, 265−270.
48. Minetti, C., Sotogia, F., Bruno, C., Scartezzini, P., Broda, P., Bado, M., Masetti, E., Mazzocco, P., Egeo, A., Donati, M. A., Volonté, D., Galbiati, F., Cordone, G., Bricarelli, F. D., Lisanti, M. P., and Zara, F. (1998) *Nat. Genet. 18*, 365−368.
49. Galbiati, F., Volonte, D., Minetti, C., Chu, J. B., and Lisanti, M. P. (1999) *J. Biol. Chem. 274* (36), 25632−25641.
50. Galbiati, F., Volonte, D., Minetti, C., Bregman, D. B., and Lisanti, M. P. (2000) *J. Biol. Chem. 275* (48), 37702−37711.
51. Steinman, R. M. (1968) *Am. J. Anat. 122* (1), 19−55.

BI020043N